

Partial Volume Correction for Perfusion Estimation from Multi-TI Arterial Spin Labelling

M. A. Chappell^{1,2}, A. R. Groves¹, B. J. MacIntosh^{1,3}, M. J. Donahue¹, P. Jezzard¹, and M. W. Woolrich¹

¹FMRIB Centre, University of Oxford, Oxford, United Kingdom, ²Institute of Biomedical Engineering, University of Oxford, Oxford, United Kingdom, ³Imaging Research, Sunnybrook Research Institute, Toronto, Canada

Introduction: Partial volume (PV) effects, arising from grey matter (GM), white matter (WM) and cerebrospinal fluid (CSF), are known to introduce errors in quantitative perfusion imaging. Furthermore, in patients where tissue atrophy is significant, quantitative perfusion errors due to PV effects may prevent accurate blood flow from being determined. While ASL spatial resolution is improving, resolutions of the order of 3 mm isotropic do not preclude PV effects [1]. Simple scaling correction based on PV estimates (PVE) derived from a structural segmentation has been used [2] and recently a linear regression (LR) correction has been proposed [3]. In LR, PVE from a local region are employed within a linear regression to separately estimate signal arising from GM and WM. However, this approach smooths the data with a kernel that is not well defined and thus whose effects on CBF images are difficult to quantify. Since WM and GM have different kinetics (both bolus arrival times and T1 values), it may be possible to separate their contributions using multi-TI ASL. However, these kinetic differences are small, making reliable separation difficult. Here, we propose a spatial PV correction approach that combines kinetic modelling with PVE constraints and adaptive spatial smoothing to produce GM perfusion estimates corrected for PV effects.

Methods: The Spatial PV method employed a probabilistic multi-TI kinetic curve fitting approach [4]. Three components: GM, WM and intra vascular (IV) blood water [6] were employed in the model, assuming no ASL difference signal contribution from the CSF:

$$\Delta M(t) = \Delta M_{IV}(t) + PV_{GM} \Delta M_{GM}(t) + PV_{WM} \Delta M_{WM}(t),$$

where the GM and WM components were scaled by their respective PVE obtained from a structural segmentation. Each component was modelled using three variables: CBF or arterial blood volume (aBV) for the IV, a bolus arrival time (BAT) and bolus duration (BD), and rapid exchange in the tissue compartment was assumed [5]. Since a relatively large number of parameters were to be fit from the data, appropriate priors were specified: For CBF adaptive spatial priors [7,8] were used, these applied smoothing to the CBF maps with an extent determined directly from the data. This is in contrast to conventional spatial smoothing that is applied as a pre-processing step using a fixed smoothing extent. For BAT and BD priors were defined by a normal distribution with a standard deviation of 0.3 and a mean of 0.5, 0.7, 1.0 s for BAT (IV<GM<WM) and 1.0 s for BD (all components, based on sequence). The IV component was subject to an Automatic Relevancy Determination prior to ensure that it was only included where supported by the evidence in the data [9].

For comparison the LR method of [3] was also employed using the following procedure: First the LR method was applied separately to each individual TI to produce separate GM and WM kinetic data. Various sizes for the LR region were considered, 5x5x1 is reported as this appeared to be a good compromise between correction and smoothing. The separate GM and WM multi-TI data were then analysed with a GM+IV or WM+IV kinetic model as appropriate, with the same priors as applied above. The key difference between our proposed spatial PV method and the LR method was thus not the kinetic model applied, but how the PVE were incorporated into the analysis. Data were also analysed using 'standard' model fitting: making the assumption of no partial volume effects using a GM+IV model without PVE.

Experimental data: Simulated data were generated using PVE from a single subject transformed into a 3x3x5 mm resolution. Three GM CBF spatial distributions were considered (Figure 1): (a) homogeneous 60 ml/100g/min, (b) sinusoidal variations of 10 ml/100g/min and (c) regions of hypo and hyper (20 and 100 ml/100g/min) CBF. WM CBF was set at 20 ml/100g/min and BAT were 0.7 and 1.0 s (GM,WM) and BD of 1.0 s. White noise was added to achieve an SNR of 100.

T1-weighted structural and resting state pulsed ASL images were also collected in four healthy subjects, having provided written consent, at 3.0T (Siemens), using a body coil for RF transmit and a 12-channel receive head coil: FAIR preparation with 3D-GRASE readout [10] (TR/TE 3110/23 ms, 3.44x3.44x5 mm, 64x64 matrix, 22 slices, 10 TIs, 10 averages). The T1-weighted images were segmented using the FSL tool FAST [11] and PVE obtained (GM, WM and CSF), these were transformed into the low resolution of the ASL images via a spline interpolation in a higher resolution intermediary before integration over the volume of the low resolution voxels. To make quantitative comparisons between the methods the mean estimated GM CBF within regions of interest (ROIs) was compared between the different analyses in a similar manner to [3]. 10 ROI were defined from those voxels that fell within a specified PVE range, where the ranges were 5-10, 10-20, 20-30 ... 90-100 %. In theory we would expect the corrected CBF to be the same in every ROI, since the true GM CBF should not be correlated with the proportion of GM in a voxel.

Results: Figure 1 shows example slices from the three simulated data sets from the various analyses. Both the proposed correction employing spatial priors and the LR approach recovered the GM CBF value. However, the spatial PV method was able to retain greater detail in the image, preserving the boundaries of the hyper/hypo CBF regions within the GM. Both correction methods were able to recover the correct mean CBF within the GM ROIs, with a very slight trend for the spatial PV method to overestimate at low GM PVE (not shown). Figure 2 shows an example slice from two of the four subjects, the spatial PV method estimates contained more detail than LR, generally both methods showed similar regional variations in GM CBF. Figure 3 shows the ROI results from the same two subjects, both correction methods predicted a GM CBF that had less variability with GM PVE than the standard analysis, although for subject 3 the LR based correction appeared to have been less effective. The mean estimated GM CBF for the spatial PV method was 1.6-1.7 times greater than a standard analyses across the four subjects, which was consistent with a 1.74-1.77 increase observed in mean GM CBF from the three simulated datasets.

Discussion: Both the LR and spatial PV methods offer some correction for PV for multi-TI ASL data. However, the proposed spatial PV method introduces less spatial smoothing and thus retains details and boundaries within the GM CBF image. Importantly the spatial PV method applies a well-defined smoothing directly to the CBF estimates, whereas LR smooths the data, and since the kinetic curve is non-linear this affects the subsequent accuracy of multi-TI curve fitting. The calculation of CBF within GM ROIs was used as a simple comparative metric that indicates that both methods are effective. This comparison, however, naturally favours methods that introduce large amounts of smoothing like LR. Both correction methods are dependent upon the accuracy of PVE and the alignment of these to the data, although the relatively low spatial resolution of ASL may make this less of a critical issue in practice.

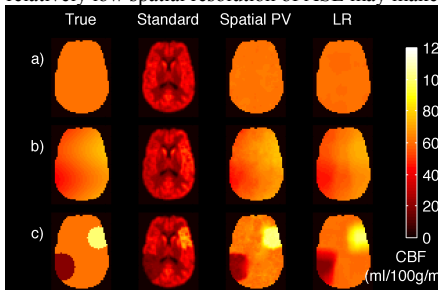


Figure 1: Simulated data showing estimated CBF for the three datasets: homogeneous (a), sinusoidally varying (b) and spatially local hyper/hypo CBF (c).

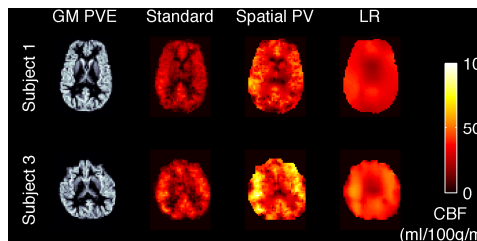


Figure 2: Example slices from two subjects, showing PVE and relative CBF images.

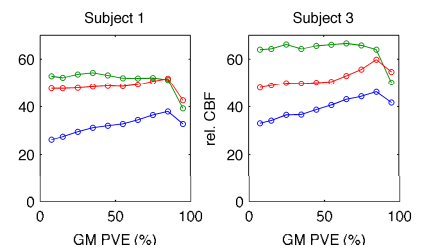


Figure 3: GM ROI analysis in two subjects, standard analysis (blue), LR corrected (red), spatial PV corrected (green).

References:

1. Donahue, M.J., *et al.*, NMR Biomed., 2006. 19:1043-1054.
2. Du, A.T., *et al.*, Neurology, 2006. 67:1215-1220.
3. Asllani, I., *et al.*, Magn. Reson. Med., 2008. 60:1362-1371.

4. Chappell, M.A., *et al.*, IEEE Trans Sig Proc, 2009. 57:223-236
5. Buxton, R.B., *et al.*, Magn Reson Med, 1998. 40:383-396
6. Chappell *et al.*, in Proc. ISMRM Hawaii, 2008.
7. Groves, A.R. *et al.*, NeuroImage, 2009. 45:795-809.

8. Penny W.D. *et al.*, NeuroImage, 2005. 24:350-362.
9. Mackay, D., Network: Computation in Neural Systems, 1995. 6:469-505.
10. Günther, M., *et al.*, Magn Reson Med, 2005. 54: p. 491-498.
11. Zhang, Y., *et al.*, IEEE Trans. Med. Imag., 2001. 20:45-57.